

# Facile Synthesis of One Dimensional AgBr@Ag Nanostructures and Their Visible Light Photocatalytic Properties

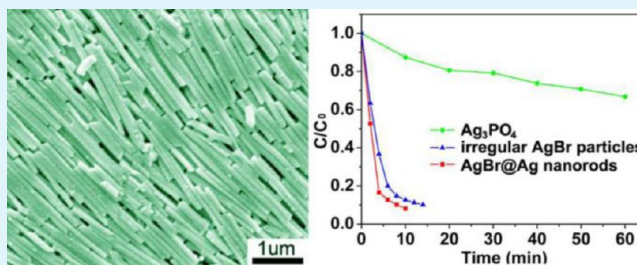
Bo Li, Hua Wang,\* Bowei Zhang, Pengfei Hu, Chang Chen, and Lin Guo\*

School of Chemistry and Environment, Beihang University, Beijing 100191, People's Republic of China

## Supporting Information

**ABSTRACT:** In this work, we successfully prepared one dimensional (1D) AgBr@Ag nanostructures in high yield by a facile wet chemical method, and the plausible growth mechanism was discussed. The synthesis of as-prepared AgBr@Ag nanostructure is a dissolution and recrystallization process, and the PVP and DMSO have a synergistic and competitive effect on the preparation of 1D AgBr@Ag products. Moreover, the AgBr@Ag nanorods exhibit excellent photocatalytic activities under visible light illumination, which may be attributed to their large surface area as well as superior charge separation and transfer efficiency compared to AgBr@Ag particles.

**KEYWORDS:** one dimension, AgBr, nanorod, photocatalyst, visible light



## INTRODUCTION

Progress in the synthesis of nano- or microstructures with controlled morphology has led to their intriguing properties and attractive applications, as well as industrial and environmental benefits. Among various nano- or microstructures, one dimensional (1D) nanostructures, including nanowires, nanorods, nanotubes, and nanobelts, have received especially intensive research interests owing to their unique electronic, optoelectronic, and electromechanical properties.<sup>1–5</sup> Facing the increasingly serious energy crisis and environmental pollution issues, using solar energy in water splitting and degradation of organic pollutants have received much attention.<sup>6–12</sup> In addition to the traditional photocatalyst TiO<sub>2</sub>, people showed a growing number of interest in some new and visible-light-responsive photocatalysts, such as BiVO<sub>4</sub>,<sup>13</sup> AgX (X = Cl, Br),<sup>14–19</sup> (Ga<sub>1–x</sub>Zn<sub>x</sub>)(N<sub>1–x</sub>O<sub>x</sub>),<sup>20</sup> Ag<sub>3</sub>PO<sub>4</sub>,<sup>21,22</sup> Ag<sub>2</sub>CrO<sub>4</sub>,<sup>23</sup> and so on. AgBr, as a high-quality photosensitive material for photography traditionally, has attracted researchers' attention recently because of its excellent visible-light-response photocatalytic performance. However, the synthesis of AgBr nanostructures with special morphologies has been rarely reported.<sup>24–27</sup> Recently, we reported the successful synthesis of AgBr polyhedra and nanoplates using simple wet chemical methods, and investigated the morphological and facet effect on its photocatalytic performance.<sup>17–19,28</sup> Ye and colleagues have developed an effective synthetic method for the preparation of AgBr 1D materials via an in-situ oxidation method, and found that AgBr core-shell nanowires revealed enhanced photocatalytic activities for MO degradation under visible light illumination.<sup>29</sup>

In this work, we reported the synthesis of 1D AgBr@Ag nanostructures in high yield by a facile wet chemical method and proposed a plausible growth mechanism. In addition, the

high efficiency of as-prepared AgBr@Ag nanorods for degradation of organic contaminants under visible light irradiation has been demonstrated.

## 2. EXPERIMENTAL SECTION

**2.1. Preparation of AgBr@Ag Nanocrystals.** In a typical precipitation reaction synthesis, 54 mg of polyvinyl pyrrolidone (PVP) (average MW 58000, K29-32, Acros) and 45 mg NaBr were added into 30 mL dimethyl sulfoxide (DMSO)/distilled water (10/20, V/V), fully dissolved. Then 10 mL CH<sub>3</sub>COOAg water solution (57 mg) was dropped to the prepared mixture solution under magnetic stirring and kept for 30 min at 60 °C. The mixture placed in a 45 mL Teflon-lined stainless steel autoclave for hydrothermal synthesis, which was conducted at 130 °C for 12 h in an electric oven. The product was washed with distilled water and dried at 60 °C under vacuum condition.

**2.2. Characterization.** The products were characterized by SEM (FEI Quanta 400, 5 KV), XRD (Rigaku Dmax 2200 X-ray diffractometer with Cu K $\alpha$  radiation), DRS (Pitachi U-3010 spectroscopy with BaSO<sub>4</sub> as reference), and BET (NOVA 2200e surface area analyzer).

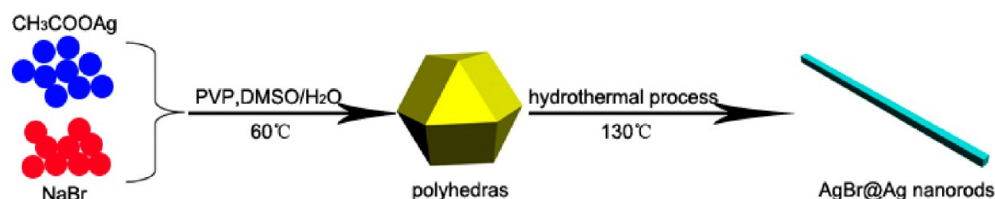
**2.3. Photocatalytic Experiment.** The photocatalytic degradation of Rhodamine B (Rh B) and methyl orange (MO) dyes was carried out in an aqueous solution at ambient temperature. A 0.1 g portion of as-prepared photocatalyst was suspended in a 100 mL Rh B (33 mg/L) or MO solution (33 mg/L). Prior to irradiation, the suspensions were magnetically stirred in the dark for 30 min to establish an adsorption/desorption equilibrium. The visible light source system consisted of a 300 W Xe lamp with UV cutoff filter (providing visible light with  $\lambda \geq 400$  nm).

Received: May 28, 2013

Accepted: November 7, 2013

Published: November 7, 2013

Scheme 1. Schematic Illustration for the Formation of the AgBr@Ag Nanorods



### 3. RESULTS AND DISCUSSION

Using DMSO and H<sub>2</sub>O as solvents, PVP as a surfactant, we prepared 1D AgBr@Ag nanocrystals by a two-step ion-exchange process. As can be shown from Scheme 1, the first step was carried out under low temperature, and the AgBr nanocrystallines were obtained as seeds for the following hydrothermal process. Figure 1A and B are typical scanning

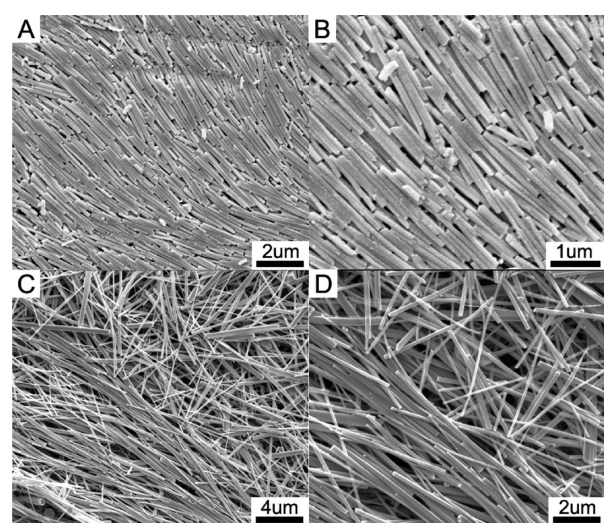


**Figure 1.** Typical scanning electron microscopy (SEM) images of the as-prepared AgBr@Ag nanorods at (A) low and (B) high magnifications and AgBr@Ag nanowires at (C) low and (D) high magnifications.

electron microscopy (SEM) images of the as-prepared AgBr@Ag products, which show that the products are composed of nanorods, which are 1.5–3 μm in length and 90–120 nm in diameter. By minor changing the experiment control, the 1D AgBr@Ag nanowires can be obtained, with length more than 6 μm and diameter smaller than 200 nm, as shown in Figure 1C and D.

By adjusting the amount of DMSO, PVP, and reaction time, we tried to study the possible growth mechanism of as-prepared AgBr@Ag nanorods. Without hydrothermal process, only irregular AgBr polyhedrons can be obtained, as shown in Figure 2A. Whereas with the increment of hydrothermal time, the AgBr polyhedrons will firstly turn small, suggesting that the AgBr crystals are dissolved. As we know, DMSO is a strong solvent that may dissolve the AgBr products, which has also been reported in other groups.<sup>30</sup> As reaction proceeds, the dissolved AgBr will recrystallize and form 1D AgBr@Ag nanostructures, as shown in Figure 2B–F. So the process is just a dissolution and recrystallization process, like the Ostwald ripening growth mechanism in the synthesis of other inorganic nanomaterials.

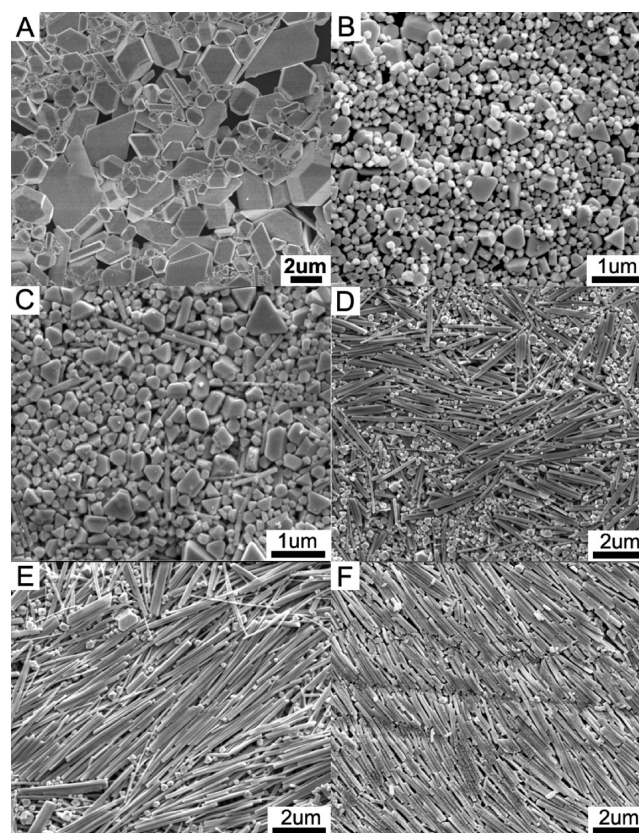


**Figure 2.** SEM images of AgBr@Ag nanorods with different reaction time: (A) without hydrothermal process; (B) 1; (C) 2; (D) 6; (E) 10; (F) 14 h.

Supporting Information Figure S11 shows the typical SEM images of as-prepared products with different amount of added PVP. It shows that with the increasing amount of the PVP added, the ratio of AgBr nanoplates with exposed {111} facets to the nanorods increased, suggesting PVP with an easily polarized functional group “—C=O” in its repeated unit can selectively adsorb on {111} facets, which is consistent with our previous report.<sup>17,31</sup> Thus, for obtaining good 1D AgBr morphologies, suitable amount of PVP is needed.

By changing the ratio of DMSO to H<sub>2</sub>O, the AgBr products evolved from small polyhedrons, through nanorods to nanowires, as shown in Figure 3. As mentioned before, DMSO can dissolve the AgBr products, so with no DMSO added, the products are polyhedrons just as the products with no hydrothermal reaction process, while with the increment of added DMSO, the AgBr polyhedrons can dissolve and recrystallize to form 1D AgBr products. Besides being a universal solvent, DMSO has an easily polarized functional group “—S=O”. “O” is negatively charged, can interact with positively charged “Ag” and stabilize the AgBr {111} facets

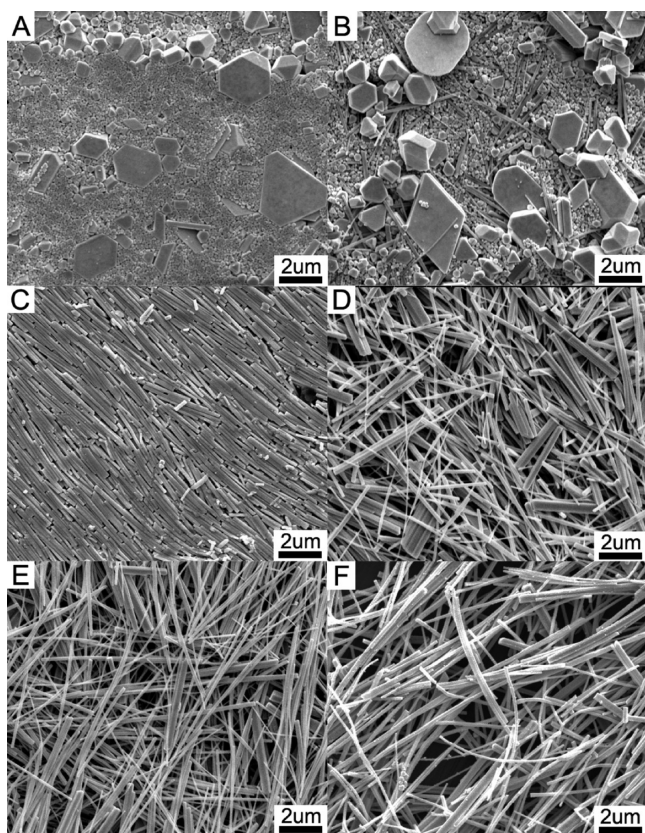


**Figure 3.** SEM images of as-prepared products with different added ratio of DMSO to H<sub>2</sub>O: (A) 0/30; (B) 5/25; (C) 10/20; (D) 15/15; (E) 20/10; (F) 25/5.

during the crystal growth process. Meanwhile, as mentioned above, PVP as a non-ionic surfactant can stabilize AgBr {111} facets, but the supramolecular interaction between DMSO and PVP exists.<sup>32–35</sup> This supramolecular interaction may weaken the adsorption capabilities of DMSO (“–S=O”) and PVP (“–C=O”) to AgBr {111} facets and strengthen the adsorption capability of N atoms in the repeated unit of PVP to AgBr {100} facets comparatively, so the 1D AgBr products may be attributed to the synergistic and competitive effect of DMSO and the PVP.

In addition, in the absence of H<sub>2</sub>O and only DMSO as the solvent, there are compositions of irregular AgBr microspheres, octahedras, and nanorods, as shown in Supporting Information Figure SI2. On the other hand, using AgNO<sub>3</sub> instead of CH<sub>3</sub>COOAg as the source of Ag<sup>+</sup> ions, it can be seen that only AgBr polyhedrons can be obtained, as shown in Figure SI2, suggesting that CH<sub>3</sub>COOAg plays a very significant role on the formation of 1D AgBr nanostructures. CH<sub>3</sub>COOAg with a low dissociation constant in DMSO not only can slow the formation of AgBr but also can facilitate the enough competitive adsorption of DMSO and PVP to the AgBr nanocrystals.

Figure 4A shows the XRD patterns of the as-prepared AgBr@Ag nanorods. We can see that the sample consists of face-centered cubic structure of AgBr (JCPDS no. 6-438) and a small amount of Ag. DMSO has weak reducibility under the high temperature, and the metal Ag should be brought by the reduction of AgBr. The UV-visible diffuse reflectance spectra of the AgBr@Ag nanorods show obvious absorption in the visible region with wavelength larger than 500 nm compared to

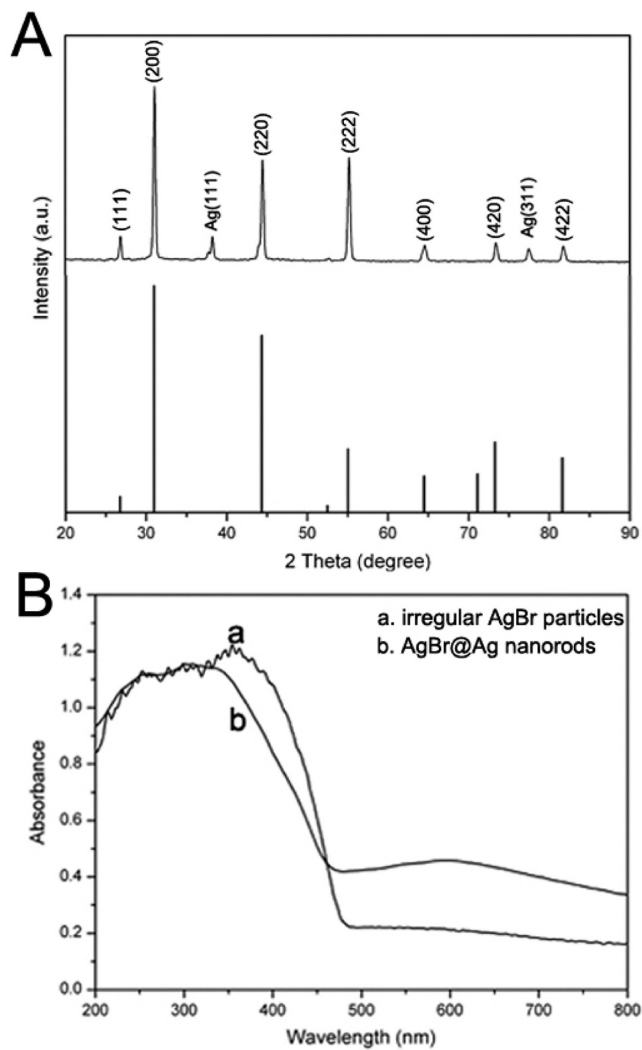


**Figure 4.** XRD patterns and typical UV–vis diffuse reflectance spectra (DRS) of as-prepared AgBr@Ag nanorods.

irregular AgBr particles, manifesting the existence of a trace amount of Ag. The corresponding XPS spectrum (Supporting Information Figure SI3) shows peaks at 367.4 and 373.4 eV, which should be assigned to Ag(I) 3d<sub>5/2</sub> and 3d<sub>3/2</sub>, while the weak XPS peaks at 367.7 and 373.7 eV are assigned to Ag(0) 3d<sub>5/2</sub> and 3d<sub>3/2</sub>, demonstrating the existence of Ag, and the phenomena are consistent with the results of DRS.<sup>19</sup> Meanwhile, the XRD and DRS of AgBr@Ag nanowires are also characterized, as shown in Supporting Information Figure SI4. It can be seen that there are some unknown peaks in the XRD pattern, suggesting the nanowire products are impure, and the DRS demonstrate that there are a trace amount of metal Ag.

The photocatalytic properties of our AgBr-based products are evaluated by photodegradation toward MO and Rh B dyes under visible-light illumination. In the contrast experiment, Ag<sub>3</sub>PO<sub>4</sub> as a new type of highly efficient photocatalysts was prepared, and its photocatalytic performance was investigated.<sup>36</sup> As shown in Figure 5A, we can see both of the AgBr-based photocatalysts have better photocatalytic performance than Ag<sub>3</sub>PO<sub>4</sub> in photodegradation of MO. Meanwhile, it can be clearly seen that the AgBr@Ag nanorods show highly photocatalytic activity, and the photodegradation rate of MO dyes over AgBr@Ag nanorods is at least 1.5 times faster than

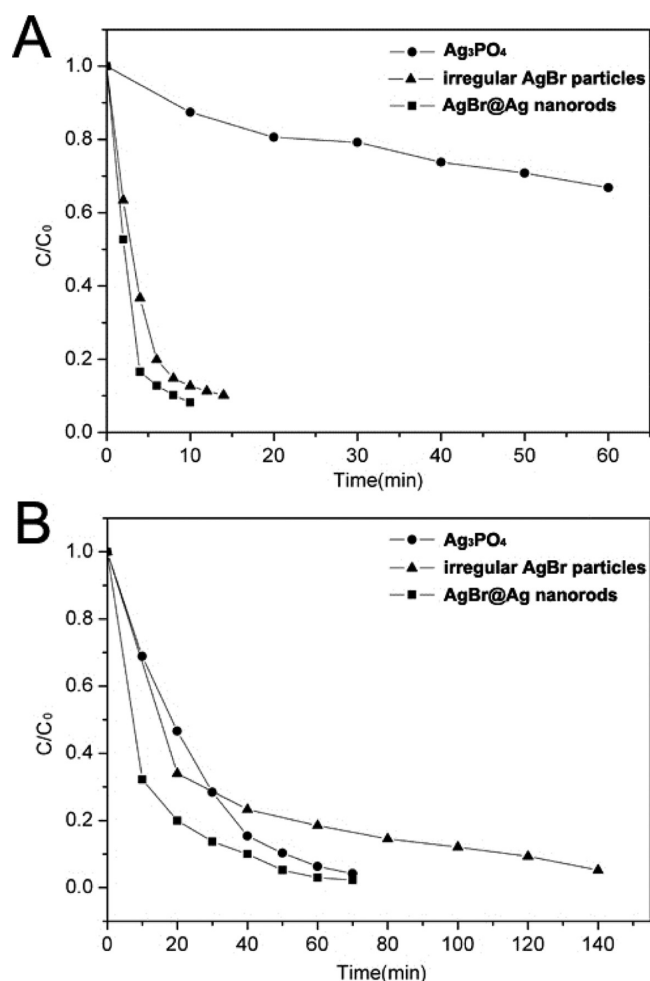


**Figure 5.** Photodegradation of MO (A) and Rh B (B) dyes over the as-prepared samples.

the irregular AgBr particles, as well as tens of times faster than the highly efficient  $\text{Ag}_3\text{PO}_4$  photocatalyst. For the photodegradation of RhB dye,  $\text{Ag}_3\text{PO}_4$  has high activities than normal AgBr particles, which may be due to its high oxidative activity of its valence band potential, whereas the AgBr@Ag nanorods have the comparable photocatalytic activities with  $\text{Ag}_3\text{PO}_4$ , as shown in Figure 5B. The Brunauer–Emmett–Teller (BET) nitrogen adsorption analysis showed that the specific surface areas of the AgBr@Ag nanorods was  $7.03 \text{ m}^2 \text{ g}^{-1}$ . The superior photocatalytic performance of AgBr@Ag nanorods should be attributed to its high surface area to provide more active sites, and its improved charge separation and transfer efficiency compared to AgBr particles. The photocatalytic properties of the as-prepared AgBr@Ag nanowires are very bad, which may be due to its impurity phase.

#### 4. CONCLUSION

In summary, we have successfully synthesized 1D AgBr@Ag nanostructure and discussed the possible growth mechanism, which is a dissolution and recrystallization progress, and the PVP and DMSO have a synergistic and competitive effect on the preparation of 1D AgBr@Ag products. Moreover, owing to the large surface area, improved charge separation, and transfer efficiency, AgBr@Ag nanorods exhibit excellent photocatalytic activities under visible light illumination.

#### ■ ASSOCIATED CONTENT

##### Supporting Information

SEM images of as-prepared products with different amount of added PVP, as well as with no  $\text{H}_2\text{O}$  added and using  $\text{AgNO}_3$  instead of  $\text{CH}_3\text{COOAg}$ . XPS spectrum of as-prepared AgBr@Ag nanorods. XRD patterns and typical UV–vis diffuse reflectance spectra (DRS) of as-prepared AgBr nanowires. This material is available free of charge via the Internet at <http://pubs.acs.org>.

#### ■ AUTHOR INFORMATION

##### Corresponding Author

\*E-mail: [guolin@buaa.edu.cn](mailto:guolin@buaa.edu.cn).

##### Notes

The authors declare no competing financial interest.

#### ■ ACKNOWLEDGMENTS

This work was supported by the National Basic Research Program of China (2010CB934700), the National Natural Science Foundation of China (51272012), and the Specialized Research Fund for the Doctoral Program of Higher Education (20111102130006).

#### ■ REFERENCES

- (1) Liang, H. W.; Liu, S.; Yu, S. H. *Adv. Mater.* **2010**, *22*, 3925–3937.
- (2) Xia, Y. N.; Yang, P. D.; Sun, Y. G.; Wu, Y. Y.; Mayers, B.; Gates, B.; Yin, Y. D.; Kim, F.; Yan, H. Q. *Adv. Mater.* **2003**, *15*, 353–389.
- (3) Huang, M. H.; Mao, S.; Feick, H.; Yan, H. Q.; Wu, Y. Y.; Kind, H.; Weber, E.; Russo, R.; Yang, P. D. *Science* **2001**, *292*, 1897–1899.
- (4) Yang, W. L.; Zhang, L.; Hu, Y.; Zhong, Y. J.; Wu, H. B.; Lou, X. W. *Angew. Chem. Int. Ed.* **2012**, *51*, 11501–11504.
- (5) Wu, H. B.; Hng, H. H.; Lou, X. W. *Adv. Mater.* **2012**, *24*, 2567–2571.
- (6) Yang, S. H.; Liu, S. J.; Hua, Z. H.; Yang, S. G. *J. Alloys Compd.* **2011**, *509*, 6946–6949.
- (7) Chen, X.; Shen, S.; Guo, L.; Mao, S. S. *Chem. Rev.* **2010**, *110*, 6503–6570.
- (8) Honda, K.; Fujishima, A. *Nature* **1972**, *238*, 37–38.
- (9) Tsuji, I.; Kato, H.; Kudo, A. *Angew. Chem. Int. Ed.* **2005**, *44*, 3565–3568.
- (10) Li, J.; Zang, J. *Coord. Chem. Rev.* **2009**, *253*, 3015–3041.
- (11) Zang, H.; Lv, X.; Li, Y.; Li, L.; Li, J. *ACS Nano* **2010**, *4*, 380–386.
- (12) Yang, W.; Zhang, L.; Hu, Y.; Zhong, Y.; Wu, H. B.; Lou, X. W. *Angew. Chem. Int. Ed.* **2012**, *51*, 11501–11504.
- (13) Kudo, A.; Ueda, K.; Kato, H.; Mikami, I. *Catal. Lett.* **1998**, *53*, 229–230.
- (14) Wang, P.; Huang, B.; Qin, X.; Zang, X.; Dai, Y.; Wei, J.; Wangbo, M. *Angew. Chem. Int. Ed.* **2008**, *47*, 7931–7933.
- (15) Wang, P.; Huang, B.; Zang, Q.; Zang, X.; Qin, X.; Dai, Y.; Zang, J.; Yu, J.; Liu, H.; Lou, X. *Chem.—Eur. J.* **2010**, *16*, 10042–10047.
- (16) An, C.; Peng, S.; Sun, Y. *Adv. Mater.* **2010**, *22*, 2570–2574.
- (17) Wang, H.; Gao, J.; Guo, T. Q.; Wang, R. M.; Guo, L.; Liu, Y.; Li, J. H. *Chem. Commun.* **2012**, *48*, 275–277.
- (18) Wang, H.; Yang, J. T.; Li, X. L.; Zhang, H. Z.; Li, J. H.; Guo, L. *Small* **2012**, *8*, 2802–2806.
- (19) Wang, H.; Li, Y.; Li, C.; He, L.; Guo, L. *CrytEngComm* **2012**, *14*, 7563–7566.
- (20) Maeda, K.; Teramura, K.; Lu, D.; Takata, T.; Saito, N.; Inoue, Y.; Domen, K. *J. Phys. Chem. B* **2006**, *110*, 13753–13758.
- (21) Yi, Z.; Ye, J.; Kikugawa, N.; Kako, T.; Quyang, S.; StuartWilliams, H.; Yang, H.; Cao, J.; Luo, W.; Liu, Y.; Withers, R. L. *Nat. Mater.* **2010**, *9*, 559–564.
- (22) Wang, H.; He, L.; Wang, L. H.; Hu, P. F.; Guo, L. *CrytEngComm* **2012**, *14*, 8342–8344.

- (23) Ouyang, S.; Li, Z. S.; Ouyang, Z.; Yu, T.; Ye, J. H.; Zou, Z. G. *J. Phys. Chem. C* **2008**, *112*, 3134–3141.
- (24) Elahifard, M. R.; Rahimnejad, S.; Haghighi, S.; Gholami, M. R. *J. Am. Chem. Soc.* **2007**, *129*, 9552–9553.
- (25) Zang, L. S.; Wong, K. H.; Yip, H. Y.; Hu, C.; Yu, J. C.; Chan, C. Y.; Wong, P. K. *Environ. Sci. Technol.* **2010**, *44*, 1392–1398.
- (26) Lou, Z. Z.; Huang, B. B.; Qin, X. Y.; Zang, X. Y.; Wang, Z. Y.; Zeng, Z. K.; Cheng, H. F.; Wang, P.; Dai, Y. *CrystEngComm* **2011**, *13*, 1789–1793.
- (27) Wang, P.; Huang, B. B.; Zang, X. Y.; Qin, X. Y.; Dai, Y.; Jin, H.; Wei, J. Y.; Wangbo, M. H. *Chem.—Eur. J.* **2009**, *15*, 1821–1824.
- (28) Wang, H.; Lang, X. F.; Gao, J.; Liu, W.; Wu, D.; Wu, Y. M.; Guo, L.; Li, J. H. *Chem.Eur. J.* **2012**, *18*, 4620–4626.
- (29) Bi, Y.; Ye, J. *Chem.—Eur. J.* **2010**, *16*, 10327–10331.
- (30) Milan, A.; Bennema, P.; Verbeeck, A.; Bollen, D. J. *Cryst. Growth* **1998**, *192*, 215–224.
- (31) Wang, H.; Liu, Y.; Hu, P. F.; He, L.; Li, J. H.; Guo, L. *ChemCatChem* **2013**, *5*, 1426–1430.
- (32) Rodriguez-Gattorno, G.; Diaz, D.; Rendon, L.; Hernandez-Sequera, G. O. *J. Phys. Chem. B* **2002**, *106*, 2482–2487.
- (33) Yount, W. C.; Loveless, D. M.; Craig, S. L. *Angew. Chem. Int. Ed.* **2005**, *44*, 2746–2748.
- (34) Loveless, D. M.; Jeon, S. L.; Craig, S. L. *J. Mater. Chem.* **2007**, *17*, 56–61.
- (35) Xu, D. H.; Liu, C. Y.; Craig, S. L. *Macromolecules* **2011**, *44*, 2343–2353.
- (36) Wang, H.; Bai, Y. S.; Yang, J. T.; Lang, X. F.; Li, J. H.; Guo, L. *Chem. Eur. J.* **2012**, *18*, 5524–5529.